44th AIAA Aerospace Sciences Meeting and Exhibit
9 - 12 January 2006, Reno, Nevada

AIAA 2006-1307

Vortex Shedding in the Near Wake of Rigid and Flexible Bluff Bodies

Kenneth J. Desabrais*
U.S. Army RDECOM – Natick Soldier Center, Natick, MA, 01760

and

Hamid Johari†
Worcester Polytechnic Institute, Worcester, MA 01609

The velocity profiles and shedding frequencies of three axisymmetric bluff bodies consisting of a disk, a cup, and a rigid canopy model were examined in the near wake, $0.25 \leq z/D \leq 9.0$. The measurements were conducted at a Reynolds number of 1.93×10^5 using a single element hot-film anemometer. The data revealed that the mean velocity deficit profiles became self-similar beyond $z/D \geq 3.0$, and are identical in self-similar coordinates. However, the cup and rigid canopy models recover more quickly than the disk. At least two shedding frequencies were observed in the near wake of these axisymmetric models; one corresponding to the dominant downstream mode at a Strouhal number ≈ 0.15 and the other at low Strouhal numbers which disappears after $z/D \geq 3.0$. The dominant mode appears at $z/D \geq 1.6$ and persists at all locations further downstream. This mode has typically been associated with a helical mode present for axisymmetric bluff bodies with a fixed separation point. A high Strouhal number mode (≈ 0.55) seen in flexible parachute canopies does not appear to be present in the near wake of these rigid models including the rigid canopy.

Nomenclature

A	=	amplitude of oscillation
D	=	model diameter
ΔU	=	velocity deficit, $\Delta U = U_\infty - U$
ΔU_m	=	maximum velocity deficiency
f	=	frequency
f_s	=	sampling frequency
h	=	model height
n	=	number of data points
r	=	radial coordinate
$r_{½}$	=	radial location where velocity deficit is ½ of the maximum
Re	=	Reynolds number, $U_\infty \cdot D / \nu$
St	=	Strouhal number, $f \cdot D / U_\infty$
S_v	=	power spectral density of the radial velocity component
u	=	axial velocity component
U	=	mean axial velocity component
u'_{rms}	=	axial velocity fluctuations
U_∞	=	freestream velocity
v	=	radial velocity component
X_v, X_v^*	=	fast Fourier transform (and its complex conjugate) of the radial velocity component

* Research Aerospace Engineer, Airdrop/Aerial Delivery, 15 Kansas Street/AMSRD-NSC-AD-AT. Member AIAA.
† Professor, Mechanical Engineering Department, 100 Institute Road. Associate Fellow AIAA.

This material is declared a work of the U.S. Government and is not subject to copyright protection in the United States.

z = downstream location from leading edge of model

ν = kinematic viscosity

I. Introduction

The main objective of this project was to study vortex shedding in the near wake of rigid axisymmetric bluff bodies having a geometry similar to an inflated, round parachute canopy. Recent experiments[1] have shown that a flexible canopy has a high frequency mode that corresponds to the canopy breathing, i.e. cyclic expansion and contraction of the canopy. On the other hand, previous work on axisymmetric rigid bluff bodies such as disk has only revealed a dominant helical mode and a very low frequency axisymmetric mode in the near wake. The present work was undertaken to assess whether a high frequency mode also exists in the immediate vicinity of a smooth cup and a rigid model with a geometry similar to an inflated parachute canopy.

Although the wake of rigid axisymmetric bluff bodies such as disk and sphere has been studied in the past, there is little known about flexible bluff bodies, such as parachute canopies. Round parachute canopies introduce difficult problems in the study of axisymmetric bluff body wakes. Two features specific to fabric canopies differentiate them from rigid bluff bodies such as cup, disk or sphere. First, fabric flexibility allows variations in the canopy geometry and the separation region spatial position. Second, there is a small mean flow through the canopy surface due to the fabric permeability, amounting to a few percent of the freestream velocity. Since the bluff body wakes are unsteady, combination of the flexible fabric geometry with the time dependent vortical flow in the near wake results in strong fluid-structure interaction. Moreover, the flow structure in the near wake is also responsible for the aerodynamic forces and moments experienced by the canopy. We are interested in comparing the flow dynamics and vortex shedding in the near wake of flexible canopies and their rigid analogues. The key flow features in the wake of disk and sphere are reviewed first to provide a basis for comparison with the results of our study.

Vortex shedding from spheres in incompressible flow has been studied extensively. Natarajan and Acrivos[2] found in their numerical study that the wake of a sphere becomes unstable at a Reynolds number of 105 and the primary unstable mode is non-axisymmetric, in accord with experimental observations. The structure of sphere wake turns out to be complex and Reynolds number dependent. Vortices form a double helix[3] or hairpin loops[4,5] in flow visualization studies at Reynolds numbers of $\sim 10^3$, whereas at Reynolds numbers of $\sim 10^4$ and beyond, the wake becomes completely turbulent with quasi-periodically spaced vortex loops or rings.[6] The primary Strouhal number associated with vortex shedding in the sphere wake in the subcritical regime is ≈ 0.2 for Reynolds numbers greater than about 10^3.[4,5,7,8] Also, there is a higher frequency mode close to the sphere at a Strouhal number that increases with Reynolds number.[7] This mode is a result of the Kelvin-Helmholtz vortices in the separated shear layer.

The flow in the near wake of a circular disk might be more representative of round canopies since the separation line is fixed at the disk edge, analogous to the location of separation line near the canopy skirt. Fuchs et al.[9] and Berger et al.[10] have investigated the flow structure in the disk wake at Reynolds numbers of $\sim 10^4$ using cross-spectral analysis at axial locations ranging from 3 and 9 disk diameters. Three instability modes have been identified: an axisymmetric oscillation of the recirculation bubble at a low Strouhal number of ≈ 0.05; a helical mode at a Strouhal number of ≈ 0.14; and a high frequency mode at a Strouhal number of 1.6 associated with the separated shear layer. The mean recirculation bubble extends to about 2.5 diameters behind the disk. The primary helical mode at Reynolds number of 10^4 in the disk wake was also confirmed by flow visualization experiments of Higuchi.[11,12] Berger et al.[10] observed the formation of axisymmetric vortex rings in the immediate vicinity of the disk in their flow visualization study using smoke. The tilting and linking of these rings in the near wake result in the helical structure.

The characteristic features of parachute canopies during various phases from deployment to terminal descent have been reviewed by Peterson, Strickland and Higuchi[13] and Strickland and Higuchi.[14] An interesting feature of the canopy dynamics during terminal descent is the 'breathing' of the canopy where the canopy diameter (typically near the skirt) oscillates about a mean value periodically. This is a result of the interaction of near wake fluid forces with the flexible, low-inertia fabric. Detailed measurements of the flow field in the near wake of flexible small-scale canopies in a low-speed tunnel have been reported by Desabrais.[15] In the close proximity of the canopy, the flow field has a mode corresponding to the canopy breathing at a Strouhal number of 0.55. A mode analogous to the helical mode observed in rigid bluff bodies was also observed in the wake of flexible canopies.

In this paper, we examine the mean flow profiles and vortex shedding in the near wake of a disk, a cup, and a rigid parachute canopy model having the same projected diameter. These results are compared with those of previous work on disk and flexible canopies. The experimental approach and the results are described below.

II. Experimental Setup

The experiments were conducted in a wind tunnel at a freestream velocity of 27.7 m/s. The freestream turbulence intensity was measured to be 1%. The wind tunnel test section had a 0.6 m square cross-section and was 2.4 m long. The temperature of the tunnel was maintained at a constant value through a heat exchanger mounted in the flow upstream of the flow straightener and contraction sections. A schematic of the experimental setup in shown in Fig. 1.

Three different models were investigated (see Fig. 2); a disk, a cup, and a rigid canopy model. All models were constructed of aluminum. The diameter of each model was $D = 0.106$ m which results in a Reynolds number based on the freestream velocity of 1.93×10^5. It is expected that the flow will be turbulent at this Reynolds number. The solid blockage of the models was 2.4% and no blockage corrections were applied to the data. The disk model was 3.2 mm thick with a rearward facing 45° chamfer giving a sharp leading edge around the disk. The cross-sectional shape of the cup and rigid canopy models were based on the mean cross-sectional shape of the 15 cm flexible canopy model in the work of Desabrais[15] as was the front projected shape of the rigid canopy model. The wall thickness of these models at the leading edge was 1.6 mm. The aspect ratio (h/D) of the cup and the rigid canopy models was 0.39 and 0.42, respectively. The models were mounted horizontally in the wind tunnel and centered. The models were supported by a 8 mm diameter by 280 mm long steel support rod which was connected to a streamlined support strut in the wind tunnel.

The flow velocity was measured in the wake of the models using a calibrated single-element hot-film anemometer. A single component of the velocity was sampled at a time. The axial component was measured by orientating the hot-film probe element perpendicular to the freestream velocity and the radial component was measured by orientating the element parallel with the freestream velocity. Each velocity component was sampled from the centerline of the model to a radial distance over twice the model diameter. The output of the anemometer was sampled using a 16-bit data acquisition system at a sampling frequency of 1 kHz with a total of 16384 sample taken at each data point.

Mean and fluctuating velocity profiles in the wake of the models were obtained from measurements of the axial velocity component. The uncertainty of the velocity measurements was estimated to be 2%. The velocity profiles were obtained at five locations from the leading edge of the models: $z/D = 0.25$, 1.0, 3.0, 6.0, and 9.0. In the very near wake ($z/D < 3.0$), flow reversal occurs in the wake directly behind the model. The shedding characteristics of the models were obtained by measuring the radial velocity component near the edge of the wake at seven downstream locations ($z/D = 0.25$, 1.0, 1.25, 1.6, 3.0, 6.0, and 9.0). The power spectral density of the radial velocity component was calculated using the Fast Fourier Transform (FFT). The uncertainty in selecting the power spectral density peaks was estimated at ±1.3 Hz which corresponds to an uncertainty in the Strouhal number of ±0.005.

III. Results

The wake profiles were examined by measuring the mean axial velocity component at the five downstream locations. The wake velocity deficit, defined as $\Delta U = U_\infty - U$, for the three models is shown in Fig. 3. The profiles of all three models show similar behavior. In the very near wake of the models ($z/D = 0.25$ and 1.0), the flow is accelerated around the body as is evident by the negative velocity deficit around the model at $0.7 \le r/D \le 1.0$). As is clearly apparent at $z/D = 0.25$, a distinct thin shear layer exists close to the edge of the body ($0.5 \le r/D \le 0.8$) which gets diffused as it grows into the fully developed wake. Directly behind the models, the flow reverses given that a recirculation bubble exists within 2.5 diameters of the disk.[10] The inversion of the profile curves in the near wake shows the ineffectiveness of the single-element hot-film to discern the direction of the fluid velocity in the recirculation bubble. Away from the model centerline, the deficit diminishes as at the velocity approaches the freestream velocity.

At downstream locations $z/D \ge 3.0$, the maximum velocity deficit on the centerline monotonically diminished ($\Delta U \to 0$) as the velocity approaches the freestream value away from the centerline. The recirculation bubble is fully closed at $z/D \ge 3.0$ and the flow has begun to recover. Both the cup and the rigid canopy models have nearly identical profiles and different from the disk. The cup and rigid canopy deficit recover more quickly than the disk. For example, at $z/D = 3.0$, the maximum deficit of the disk is 0.5 whereas the cup has already achieved a deficit recovery of 0.4. This is consistent at the axial locations further downstream as well.

The rms-value of the axial velocity fluctuations is plotted as a function of radial locations in Fig. 4 for each of the three models. The maximum rms-values are achieved in the vicinity of the shear layer being formed near the edge of the body. Maximum values are 25-30% of the freestream velocity in the shear layer and decays rapidly further downstream from the body. Far away from the centerline at all downstream locations, the axial fluctuations

approach the freestream turbulence intensity levels. The location of the peak u'_{rms} values move radially outward as the probe location goes from $z/D = 3.0$ for the cup and canopy models.

It is well known that wakes become self-similar at locations far downstream from the body. The similarity characteristics of the mean wake profiles were examined for $z/D \geq 3.0$ and the results are shown in Fig. 5. The proper normalization requires the velocity deficit, ΔU, to be normalized by the maximum deficit, ΔU_m, and the radial location be normalized by the half-width $r_{½}$ (i.e. the radial location where ½ of the maximum deficit occurs). The wakes for all three models are clearly self-similar at these downstream locations given that all the data collapses together. Similarly, there is no difference between the models either suggesting that once the flow becomes self-similar, the wake becomes independent of the shape of the body.

The vortex shedding characteristics of the models was assessed by calculating the power spectral density of the radial velocity component on the edge of the wake at seven downstream locations. A sample of the power spectral density for the rigid canopy model is shown in Fig. 6 where the power spectral density is calculated by

$$S_v = \frac{X_v^* X_v}{n \cdot f_s}$$

where X_v is the FFT of the radial velocity, X_v^* is its complex conjugate, n is the number of data points, and f_s is the sampling frequency. The power spectral density sampling locations in the wake are listed in Table 1.

Table 1. Radial probe locations for sampling the power spectral density.

z/D	*r/D*
0.25	0.69
1.0	0.81
1.25	0.81
1.6	0.81
3.0	0.75
6.0	0.84
9.0	0.84

These locations were selected in order to match the probing locations of previous research in vortex shedding characteristics of disks and flexible canopies.[1,9,10] The primary shedding frequencies were selected from examination of the FFT of the radial velocity component at each location. The shedding frequencies are stated in terms of Strouhal numbers based on the model diameter and the freestream velocity.

The shedding frequencies of the disk are plotted in Fig. 7. In the very near wake ($z/D \leq 3.0$), three distinct shedding frequency are evident, $St \approx 0.02$, 0.07, and 0.15. Both low frequency modes are of comparable amplitude (at the downstream locations where these modes are present) in the power spectral density suggesting they contain approximately equal amounts of energy in their structures. These modes are no longer present at downstream location beyond $z/D > 3.0$. Neither of these low frequency modes has been reported in the past; however, Berger et al.[10] have observed a low frequency mode at $St = 0.05$ exists which corresponds to the oscillation or pumping of the recirculation bubble. Without flow field measurements or flow visualization it is difficult to ascertain the source of the low frequency modes. The mode corresponding to $St \approx 0.15$ correlates well with a mode reported by both Fuchs et al.[9] and Berger et al.[10] which has been associated with a helical shedding mode at farther downstream locations. This mode is first detected at $z/D = 1.6$ and becomes the primary mode at all downstream locations beyond this point.

Examination of the vortex shedding of the other two models shows similar characteristics as that of the disk. Figure 8 shows the Strouhal number for all three models in addition to the primary shedding frequencies of a flexible canopy with the same mean projected diameter as the rigid models. The same dominant shedding modes at $St \approx 0.15$ observed from the disk are also observed with the cup and rigid canopy models. This mode becomes detectable as early as z/D = 1.25 for both the cup and the rigid canopy and persists at all farther downstream locations. When compared to a flexible parachute canopy, the rigid models have no vortex shedding mode which corresponds to the flexible canopy mode at $St \approx 0.55$. This suggests the latter, which corresponds to the canopy breathing, is not a natural frequency of the rigid canopy geometry but instead is a result of the fluid-structure interaction of the flexible canopy.

To further examine the development of the dominant shedding frequency at $St \approx 0.15$, the amplitude of the power spectral density peak corresponding to this mode was plotted as a function axial distance from the model leading edge. The data indicates that the mode is initiated at $z/D \approx 1.6$ and its amplitude reaches a peak value for all

three models at $z/D \approx 3.0$. The power spectral density amplitude diminishes further downstream. The reduction in the amplitude is partly due to the reduced wake strength as indicated by the decreasing turbulent fluctuations. To compensate for this effect, the amplitude of the power spectral density was normalized by the maximum velocity deficit, ΔU_m, and model diameter, D. For the positions $z/D < 3.0$, ΔU_m was taken to be U_∞. The normalized data in Fig. 9b reveals that although the amplitude of this mode increases rapidly between $z/D = 1.6$ to 3.0 and than decreases slowly further downstream.

IV. Conclusions

The velocity profiles and shedding frequencies of three axisymmetric bluff bodies consisting of a disk, cup, and rigid canopy model were examined in the near wake, $0.25 \leq z/D \leq 9.0$. The measurements were conducted at a Reynolds number of 1.93×10^5 and used single element hot-film anemometer. The data revealed that the mean velocity deficit profiles became self-similar beyond $z/D \geq 3.0$, and these profiles in self-similar coordinates are identical. However, the cup and rigid canopy models recover more quickly than the disk. The rms-values of the axial velocity fluctuations are also nearly identical for the cup and rigid canopy.

At least two shedding frequencies were observed in the near wake of these axisymmetric models; one corresponding to the dominant downstream mode at $St \approx 0.15$ and the other at low Strouhal numbers. The lower Strouhal number mode disappears after $z/D \geq 3.0$, where the $St \approx 0.15$ mode becomes the only mode. The $St \approx 0.15$ mode which has been observed previously in disk studies appears after the $z/D \approx 1.6$ and persists at all positions further downstream. Apparently, this mode is the dominant helical mode present for all axisymmetric objects with a fixed separation point, i.e. disk, cup, rigid and flexible canopies. On the other hand, the high Strouhal number mode ($St \approx 0.55$) associated with flexible canopies does not exist in the near wake of rigid models.

References

[1]Johari, H. and Desabrais, K.J., "Vortex Shedding in the Near Wake of a Parachute," *Journal of Fluid Mechanics*, Vol. 536, 2005, pp. 185-207.

[2] Natarjan, R. and Acrivos, A., "The Instability of the Steady Flow Past Spheres and Disks," *Journal of Fluid Mechanics*, Vol. 254, 1993, pp. 323-3344.

[3]Pao, H-P. and Kao, T. W., "Vortex Structure in the Wake of a Sphere," *Physics of Fluids*, Vol. 20, No. 2, 1977, pp. 187-191.

[4]Achenbach, E., "Vortex Shedding from Spheres," *Journal of Fluid Mechanics*, Vol. 62, 1974, pp. 209-221.

[5]Sakamoto, H. and Haniu, H., "A Study of Vortex Shedding from Spheres in a Uniform Flow," *Trans. ASME Journal of Fluids Engineering*, Vol. 112, 1990, pp. 386-392.

[6]Taneda, S., "Visual Observations of the Flow Past a Sphere at Reynolds Numbers Between 10^4 and 10^6," *Journal of Fluid Mechanics*, Vol. 85, 1978, pp. 187-192.

[7]Kim, H. J. and Durbin, P. A., "Observations of the Frequencies in a Sphere Wake and of Drag Increase by Acoustic Excitation," *Physics of Fluids*, Vol. 31, No. 11, 1988, pp. 3260-3265.

[8]Constantinescu G. and Squires, K., "Numerical Investigation of Flow over a Sphere in the Subcritical and Supercritical Regimes, Physics of Fluids, Vol. 16, No. 5, 2004, pp. 1449-1466.

[9]Fuchs, H. V., Mercker, E. and Michel, U., "Large-scale Coherent Structures in the Wake of Axisymmetric Bodies," *Journal of Fluid Mechanics*, Vol. 93, 1979, pp. 185-207.

[10]Berger, E., Scholz, D. and Schumm, M., "Coherent Vortex Structures in the Wake of a Sphere and a Circular Disk at Rest and Under Forced Vibrations," *Journal of Fluids and Structures*, Vol. 4, No. 3, 1990, pp. 231-257.

[11] Higuchi, H., "Visual Study on Wakes Behind Solid and Slotted Axisymmetric Bluff Bodies," *Journal of Aircraft,* Vol. 28, No. 7, 1991, pp. 427-430.

[12]Balligand, H. and Higuchi, H., "Experimental Investigation of the Wake Behind a Solid Disk," Sandia Report, SAND 90-7083, Dec., 1993.

[13]Peterson, C.W., Strickland, J.H., and Higuchi, H., "The Fluid Dynamics of Parachute Inflation," *Annual Review of Mechanics*, Vol. 28, 1996, pp. 361-387.

[14]Strickland, J. H. and Higuchi, H., "Parachute aerodynamics: An assessment of prediction capability," *Journal of Aircraft*, Vol. 33, No. 2, 1996, pp. 241-252.

[15]Desabrais, K.J., "Velocity Field Measurements in the Near Wake of a Parachute Canopy," Ph.D. Dissertation, Mechanical Engineering Dept., Worcester Polytechnic Institute, Worcester, MA, 2002.

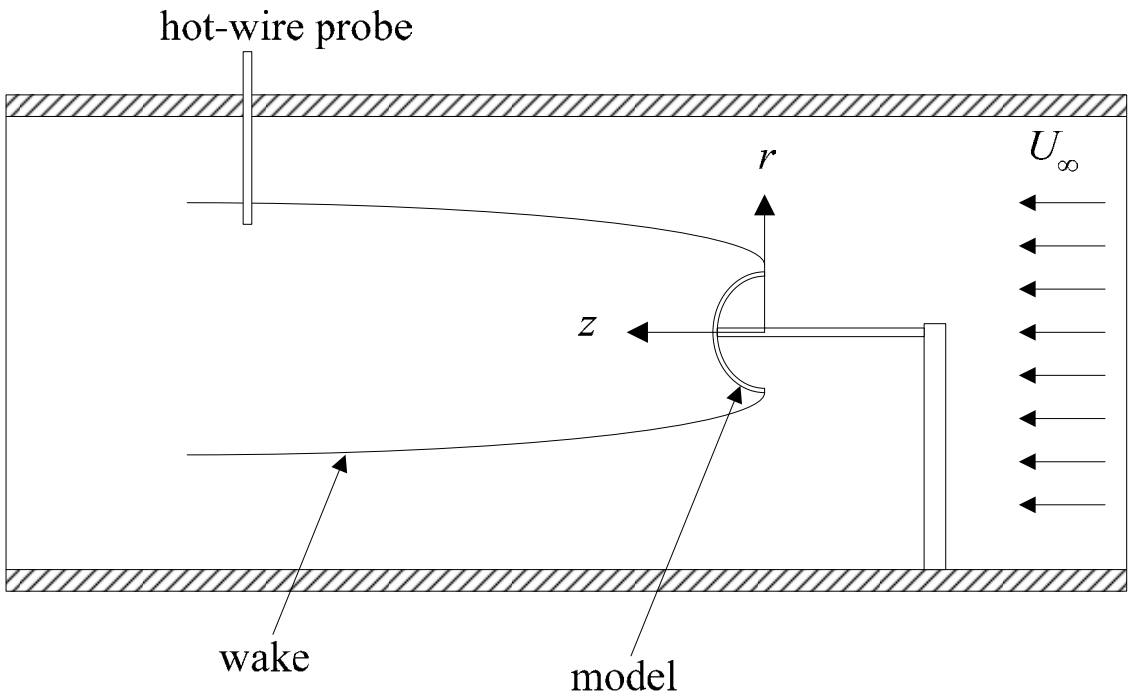

Figure 1. Schematic of experimental setup.

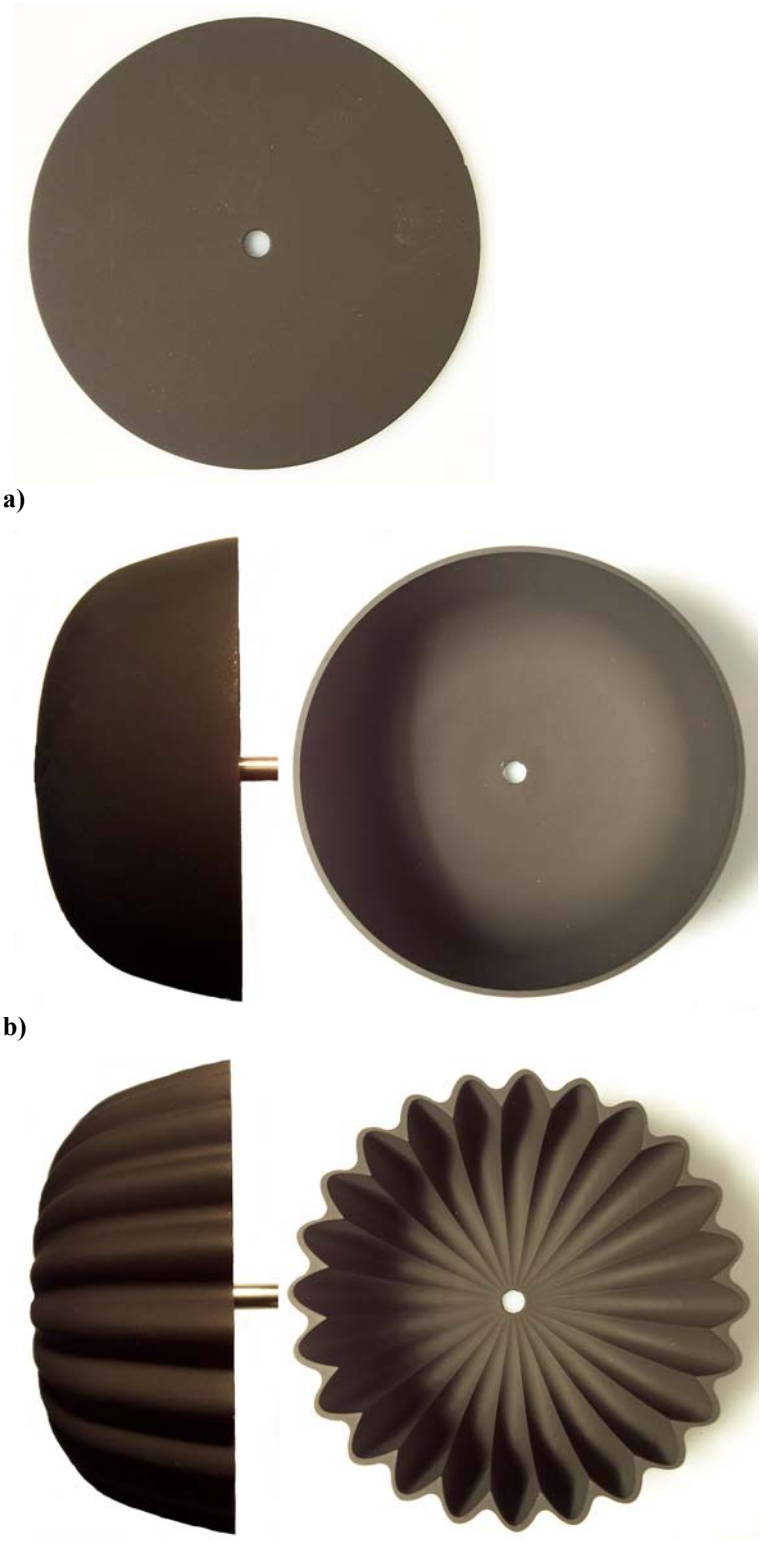

a)

b)

c)

Figure 2. Photograph of a) disk; b) cup; c) rigid canopy.

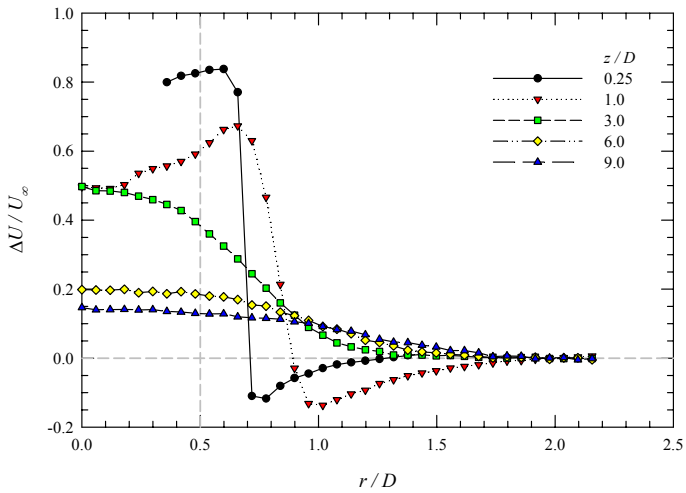

a)

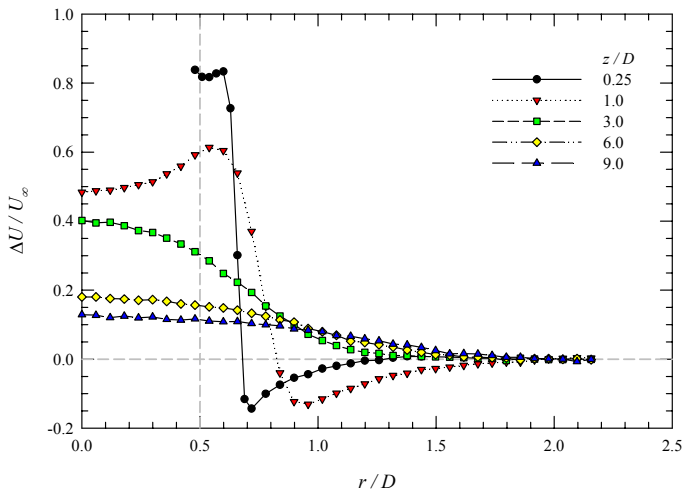

b)

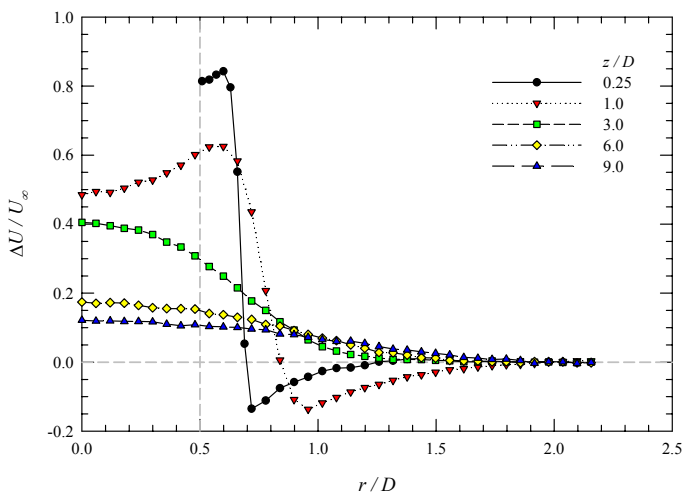

c)

Figure 3. Mean velocity deficit in the wake of a) disk; b) cup; and c) rigid canopy.

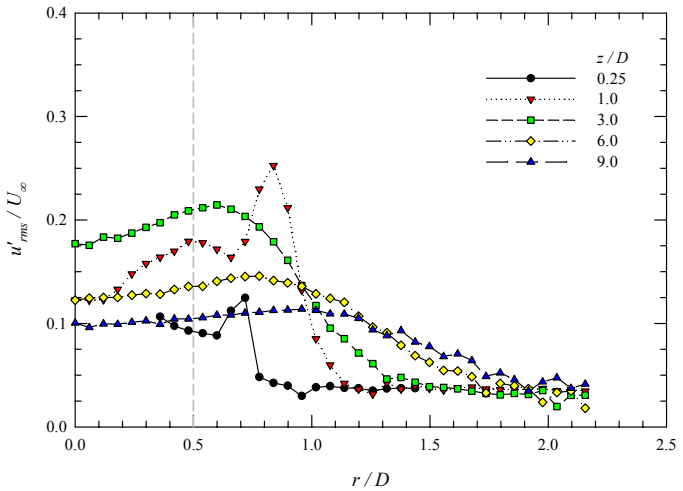

a)

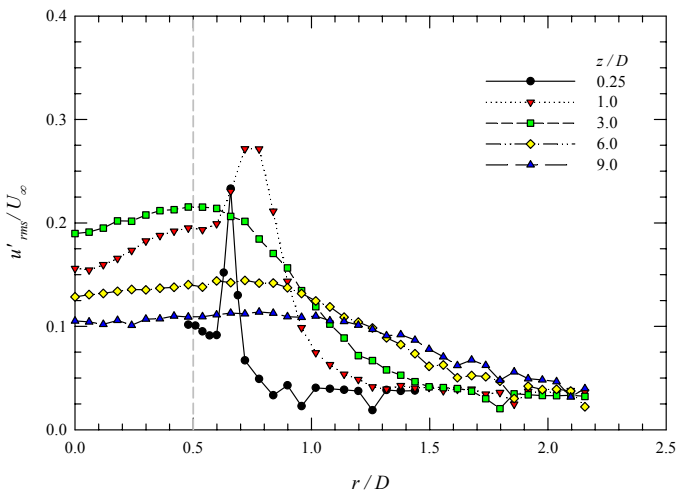

b)

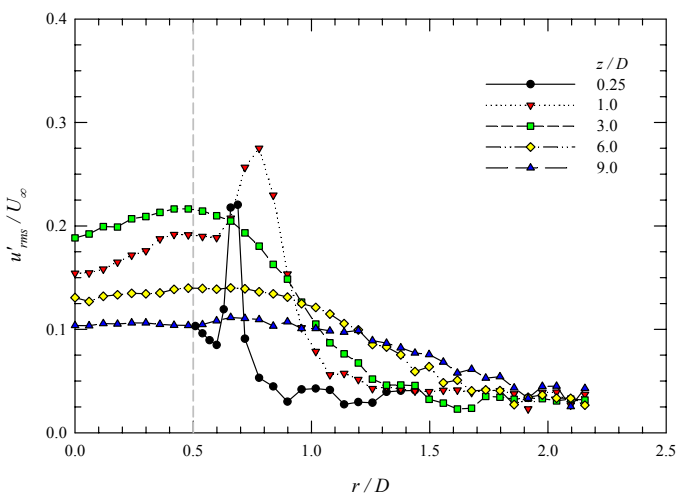

c)

Figure 4. Axial velocity fluctuations in the wake of a) disk; b) cup; and c) rigid canopy.

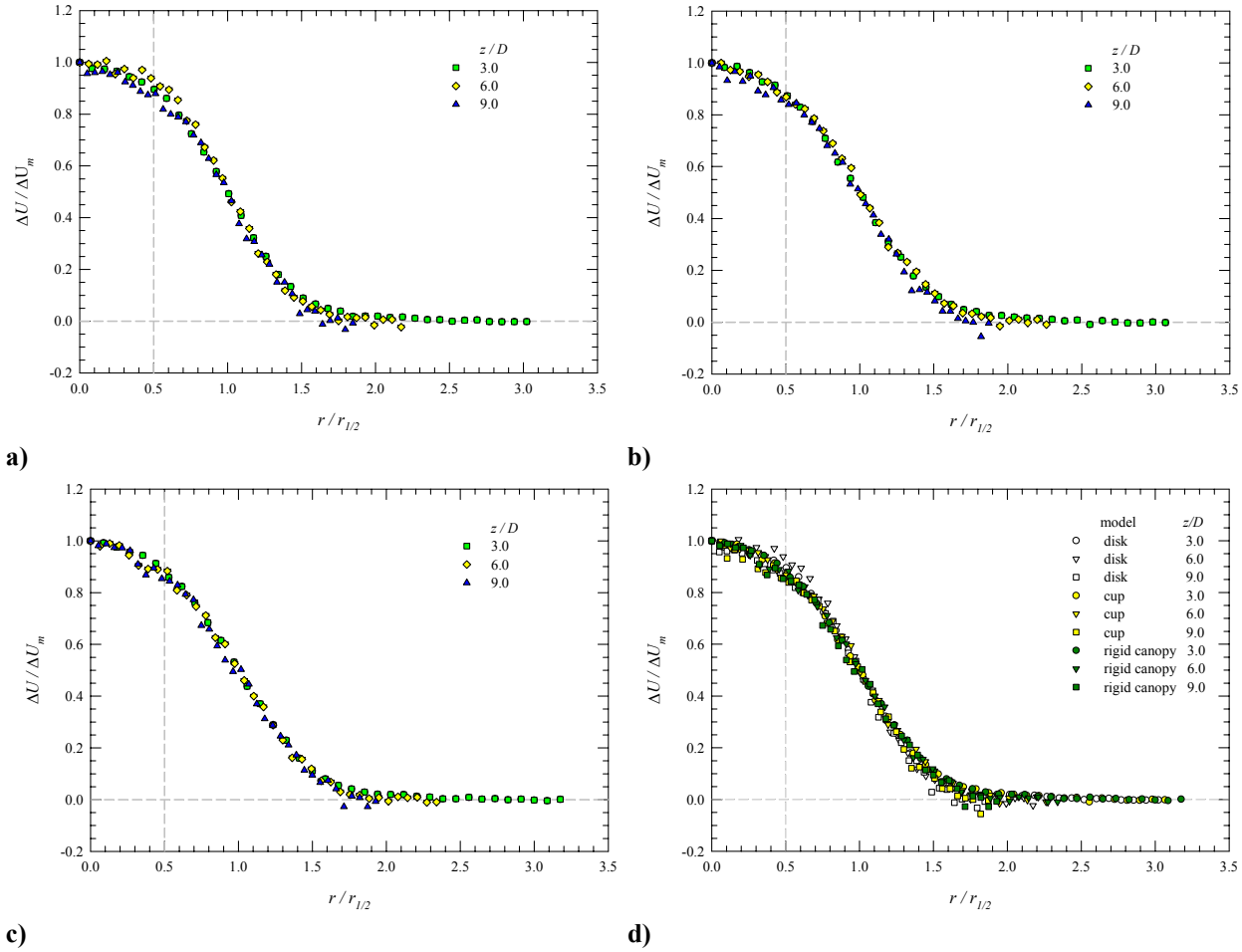

Figure 5. Similarity of axial velocity in the wake of a) disk; b) cup; c) rigid canopy; and d) all three models.

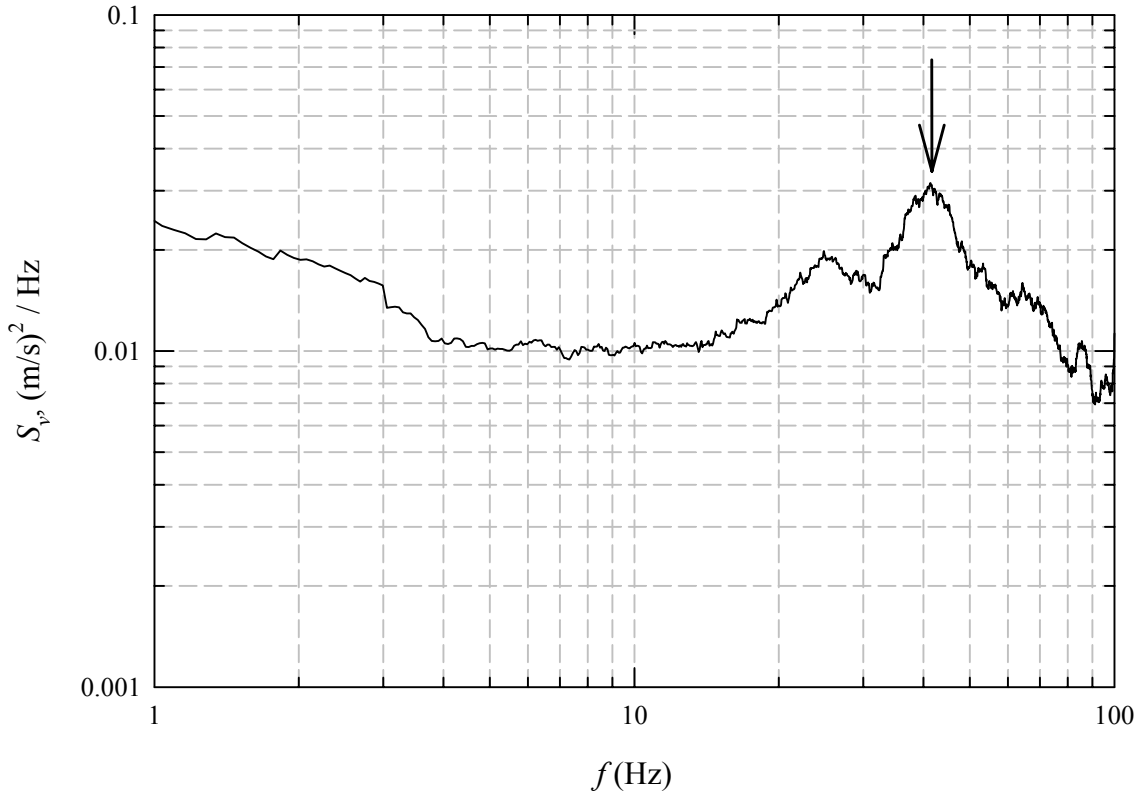

Figure 6. Sample power spectral density of radial velocity for the rigid canopy at *z/D* = 6.0, *r/D* = 0.84, and *Re* = 1.9 × 10^5. The dominant mode at *f* = 41 Hz is indicated by an arrow and corresponds to a Strouhal number of 0.157.

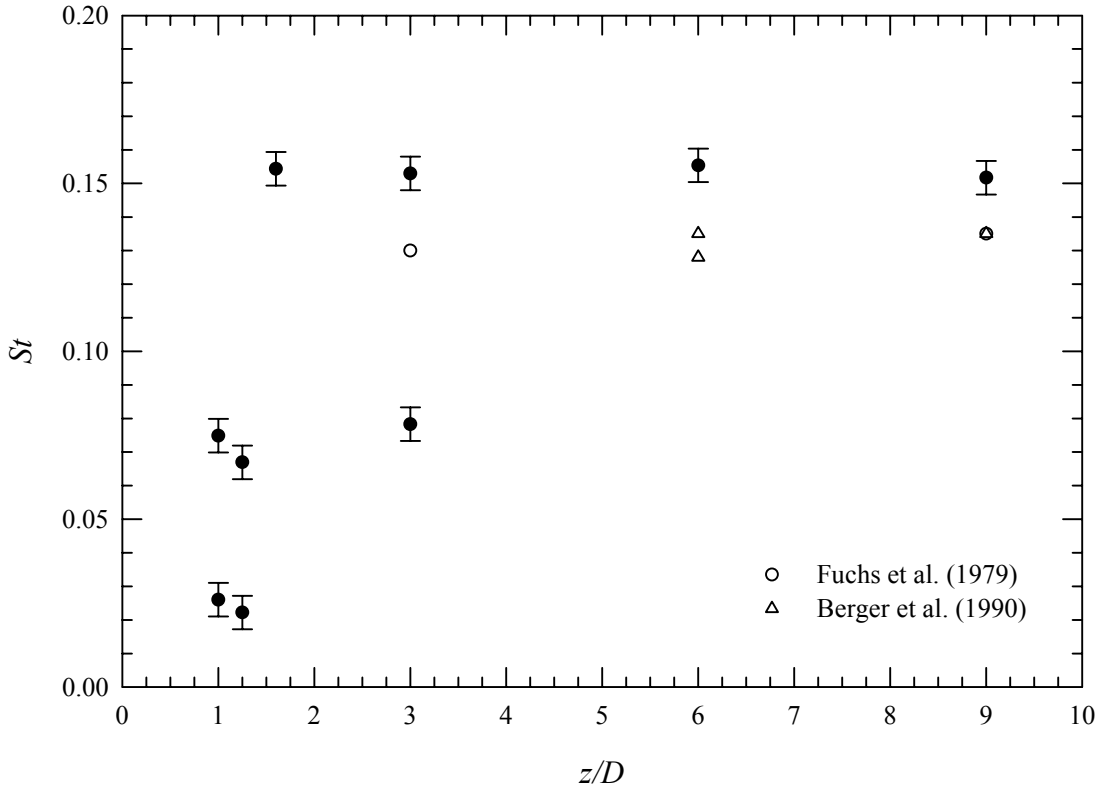

Figure 7. Shedding modes as a function of downstream location in the wake of a disk model.

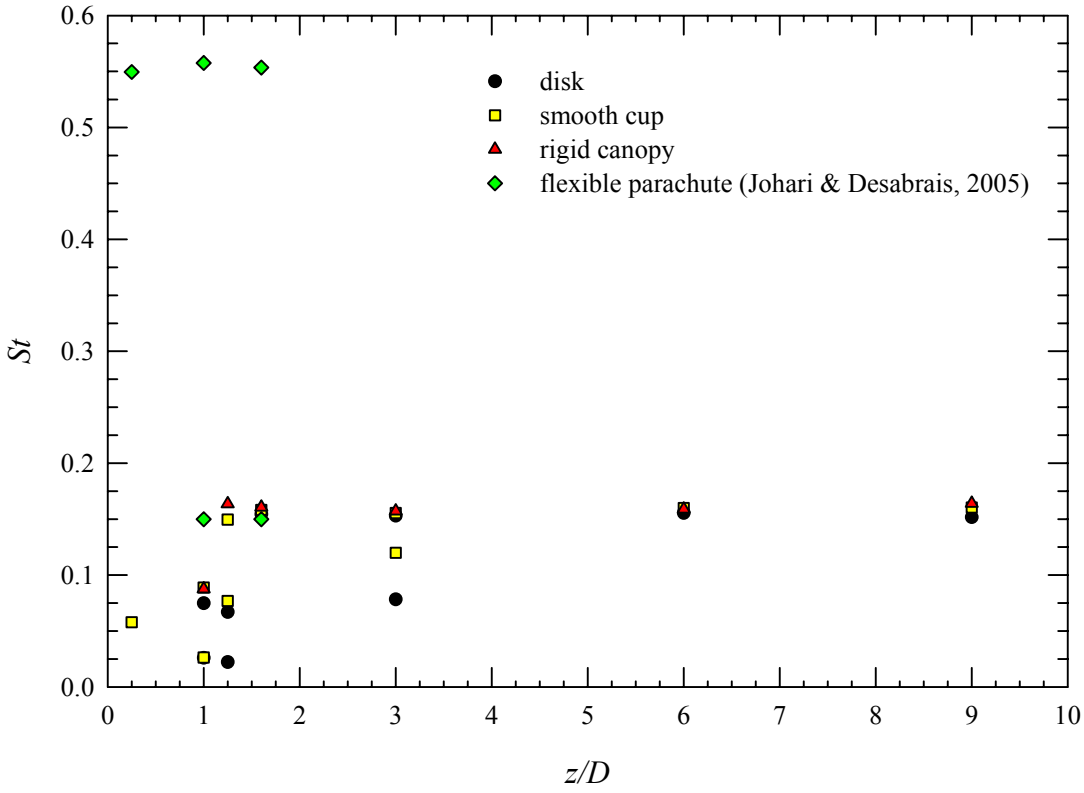

Figure 8. Shedding frequencies as a function of downstream location for all models.

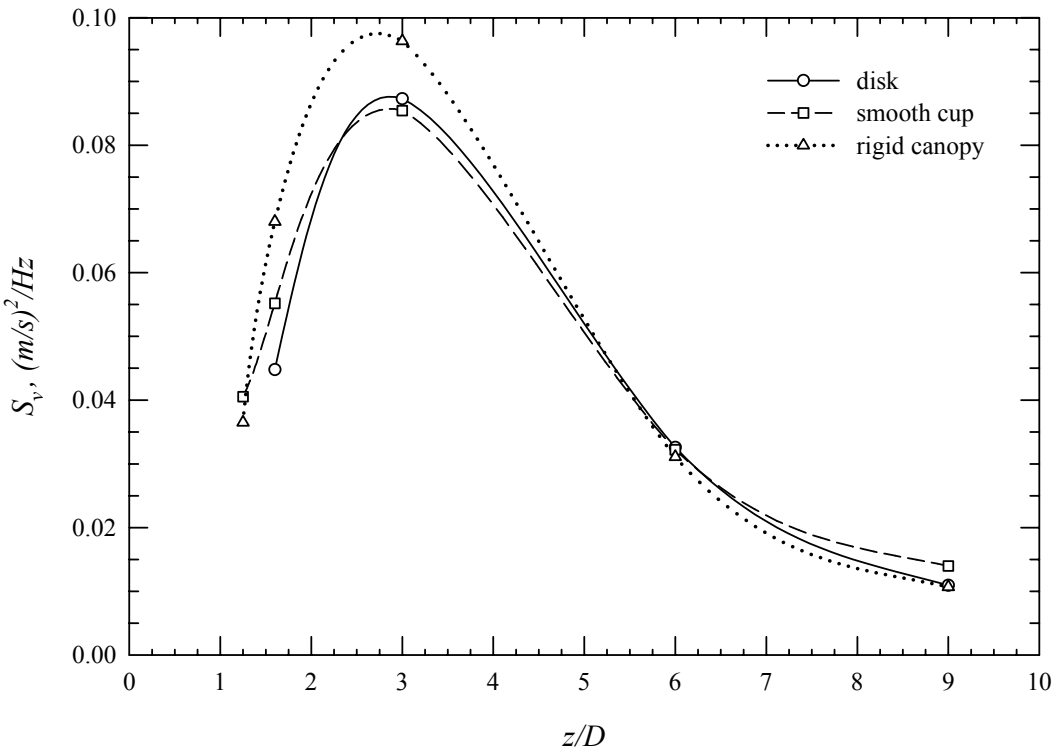

a)

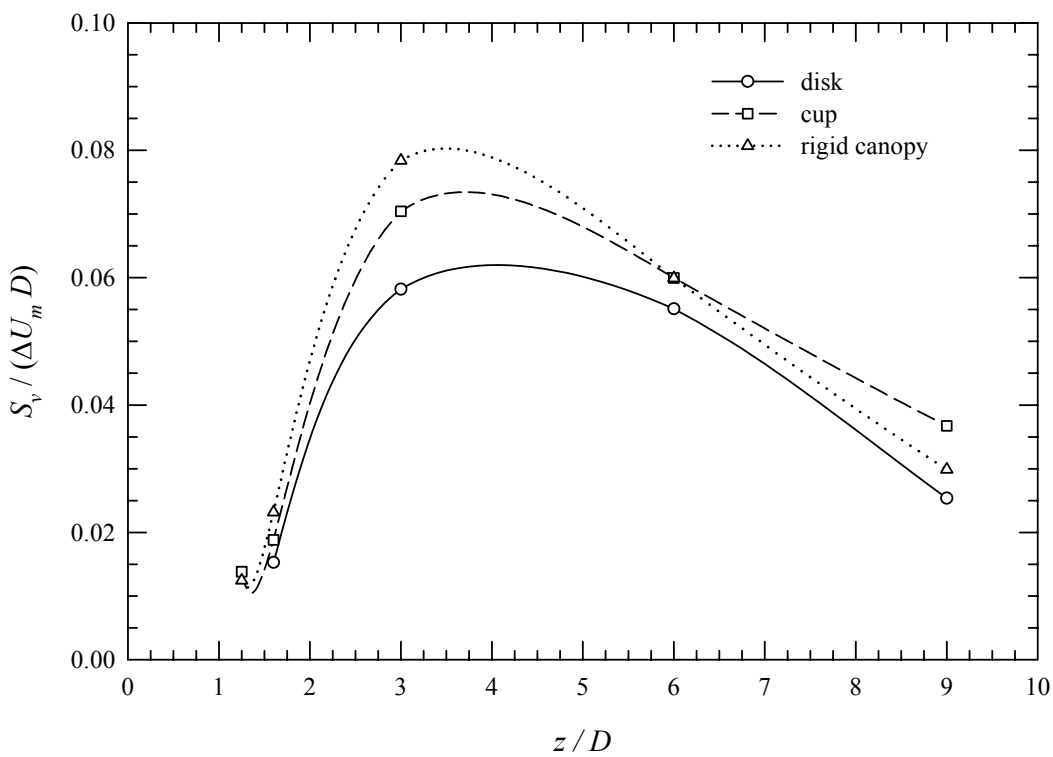

b)

Figure 9. a) Power spectral density amplitude of the helical shedding mode as a function of downstream location; b) normalized power spectral density amplitude. For $z/D < 3.0$, ΔU_m was taken to be U_∞.